



FORTH
INSTITUTE OF COMPUTER SCIENCE



H.F.R.I.
Hellenic Foundation for
Research & Innovation

GERT
GENERAL SECRETARIAT FOR
RESEARCH AND TECHNOLOGY

Tensor modeling for hyperspectral data

Anastasia Aidini

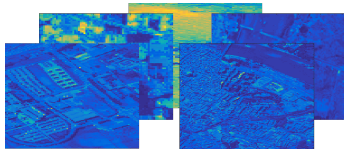
12/07/2018

DEDALE Meeting
Institute of Computer Science FORTH, Greece

Hyperspectral Images

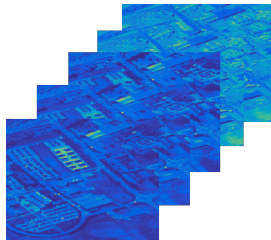
Several applications:

- astronomy
- agriculture
- biomedical imaging



Whereas the human eye sees color of visible light in mostly three bands, spectral imaging divides the spectrum into many more bands beyond the visible.

The hyperspectral images can be modeled as third-order tensors defined by two indices for spatial variables and one index for the spectral dimension.



Tensors

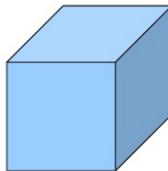
A tensor $\mathcal{X} \in \mathbb{R}^{I_1 \times I_2 \times \dots \times I_N}$ is a N -way array, a higher-order generalization of vectors and matrices.



1d-tensor



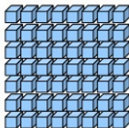
2d-tensor



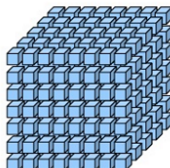
3d-tensor



4d-tensor



5d-tensor



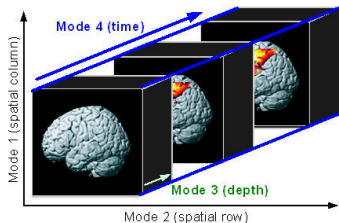
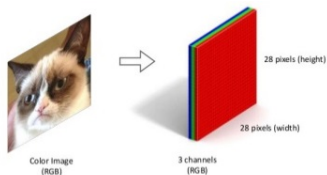
6d-tensor

Examples

- Color image - 3D tensor:
spacial variables/color
- Color video - 4D tensor:
spacial variables/color/time



- fMRI (neuro-imaging) - 4D tensor:
spacial variables/depth/time



Slices and Fibers

- *Slices* are two-dimensional sections of a tensor, defined by fixing all but two indices.
- *Fibers* are defined by fixing every index but one.

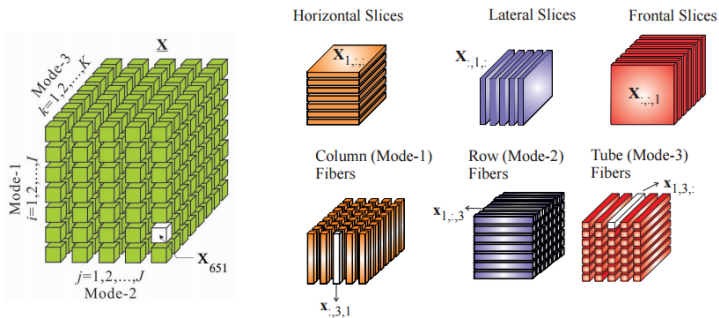


Figure: Fibers and slices of the 3d-tensor $\mathcal{X} \in \mathbb{R}^{7 \times 5 \times 8}$

Tensor Unfoldings

The mode- k unfolded matrix $X_{(k)} \in \mathbb{R}^{I_k \times \prod_{i \neq k} I_i}$ corresponds to a matrix with columns being the vectors obtained by fixing all indices of \mathcal{X} except the k -th index.

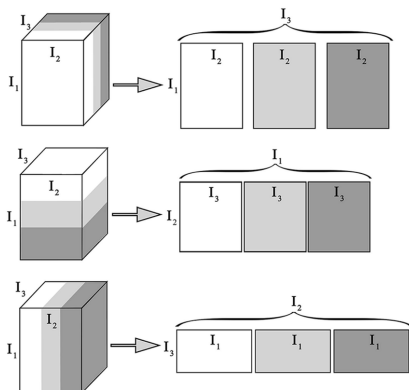


Figure: Illustration of unfolding a third-order tensor in terms of different modes.

Tensor Rank

Every tensor can be written as a sum of rank-1 tensors

$$\mathcal{X} \approx \sum_{r=1}^R a_r^{(1)} \circ a_r^{(2)} \circ \dots \circ a_r^{(N)}$$

- The *rank* of a N -way tensor \mathcal{X} is the smallest number R of rank-1 tensors needed to synthesize \mathcal{X} .
- No straightforward algorithm to determine the rank of a specific given tensor (NP-hard problem).
- The n -rank of an arbitrary N th-order tensor \mathcal{X} is the tuple of the ranks of the N unfolding matrices.

CP Decomposition

CANDECOMP/PARAFAC (CP) decomposition represents a N -order tensor $\mathcal{X} \in \mathbb{R}^{I_1 \times \dots \times I_N}$ as a linear combination of rank-1 tensors in the form

$$\mathcal{X} = \sum_{r=1}^R \lambda_r a_r^{(1)} \circ a_r^{(2)} \circ \dots \circ a_r^{(N)}$$

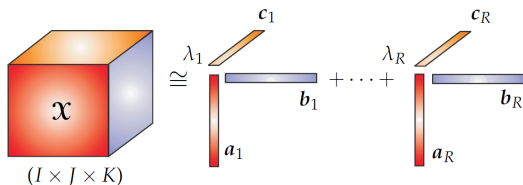


Figure: CP decomposition of the 3-order tensor $\mathcal{X} \in \mathbb{R}^{I \times J \times K}$.

CP decomposition of a tensor is unique iff the R rank-1 terms in its decomposition are unique.

Tucker Decomposition

The Tucker decomposition decomposes a N -order tensor $\mathcal{X} \in \mathbb{R}^{I_1 \times \dots \times I_N}$ into a core tensor $\mathcal{G} \in \mathbb{R}^{R_1 \times R_2 \times \dots \times R_N}$ and multiple matrices $A^{(n)} \in \mathbb{R}^{I_n \times R_n}$ which correspond to different core scaling along each mode in the form

$$\mathcal{X} = \mathcal{G} \times_1 A^{(1)} \times_2 A^{(2)} \times_3 \dots \times_N A^{(N)}$$

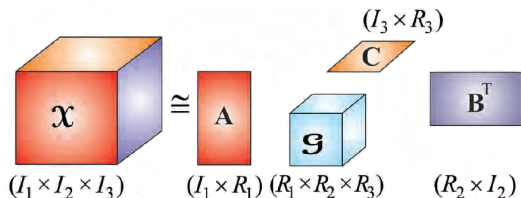


Figure: Tucker decomposition of the 3-order tensor $\mathcal{X} \in \mathbb{R}^{I_1 \times I_2 \times I_3}$.

The Tucker decomposition is in general not unique, that is, factor matrices $A^{(n)}$ are rotation invariant.

Compression of Hyperspectral Images

- Huge amount of data is collected by hyperspectral sensors.
- Compression is an important and challenging task for many applications.

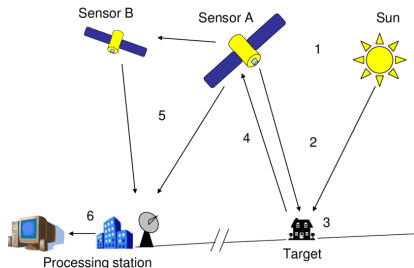


Figure: Remote sensing process.

- Compression algorithms have to take into consideration the redundancies in the spatial and spectral domains.

Lossy and Lossless Compression

Lossless compression

- reduces bits by identifying and eliminating statistical redundancy
- no information is lost
- limited compression ratio

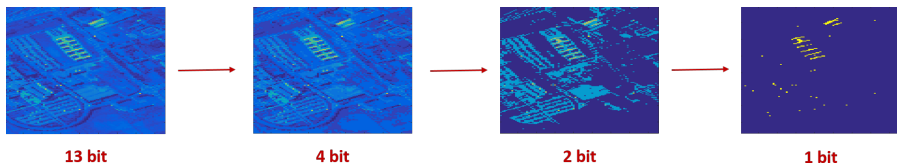
Lossy compression

- reduces bits by removing unnecessary or less important information
- higher compression ratio

Quantization

The process of mapping input values from a large set to output values in a smaller set with a finite number of bits.

- Integral part of data acquisition
 - Remote sensing scenario
 - Energy-limited systems
- Data compression

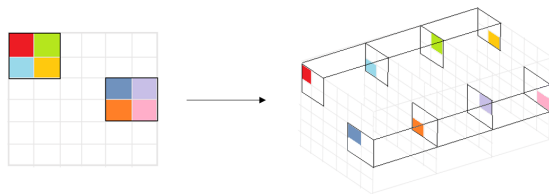


Huffman Coding

- Huffman coding is commonly used for lossless data compression.
- Huffman codes have the minimum average length (number of bits needed) as compared to all other codes.
- A Huffman code dictionary associates each data symbol with a codeword.
- A Huffman code is generated by calculating the probabilities of the source symbols and the corresponding efficiency-indices so that the resultant code is minimized in length.
- No codeword in the dictionary is a prefix of any other codeword in the dictionary.

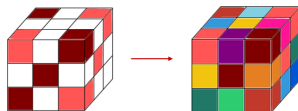
Missing measurements

- communication failures \rightarrow packets are lost
- de-synchronization of sensors \rightarrow different sampling instances
- Snapshot mosaic (SSM) imaging sensors

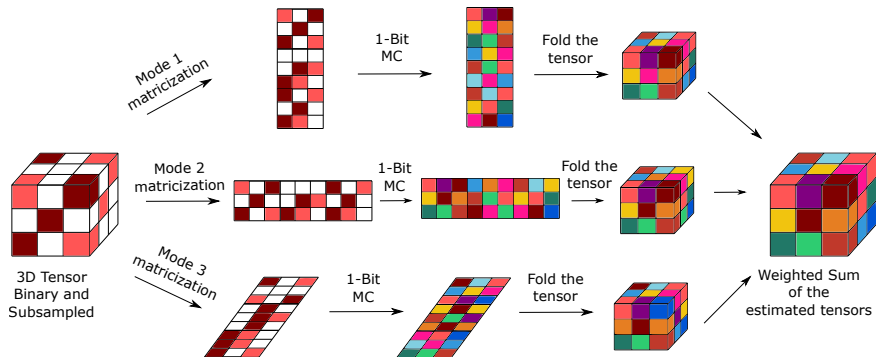


Problem

- Recovery of the real-valued entries of a tensor from a number of quantized observations
- No prior work examines the interaction between quantization and sampling in high-order structured data



The proposed method



From tensor to matrices

$\mathcal{M} \in \mathbb{R}^{I_1 \times \dots \times I_N}$ is the unknown, low-rank tensor.

$\mathbf{M}_{(n)} \in \mathbb{R}^{I_n \times \prod_{j \neq n} I_j}$ the mode- n matricization (unfolding) of the tensor \mathcal{M}

Optimization problem of matrix completion:

$$\begin{aligned} & \text{minimize}_{\mathbf{Z}_{(n)}} \text{rank}(\mathbf{Z}_{(n)}) \\ & \text{subject to } \mathcal{P}_{\Omega}(\mathbf{Z}_{(n)}) = \mathcal{P}_{\Omega}(\mathbf{M}_{(n)}) \end{aligned}$$

where \mathcal{P}_{Ω} is a random sampling operator and $\Omega \subseteq \{1, \dots, I_1\} \times \dots \times \{1, \dots, I_N\}$ the sampling set. The rank function can be replaced by the nuclear norm $\|\mathbf{Z}_{(n)}\|_*$, which is the sum of singular values of $\mathbf{Z}_{(n)}$.

Quantization model

The quantized measurement of the (i_1, \dots, i_N) – *th* entry of \mathcal{M} is

$$\begin{aligned} \mathcal{Y}_{i_1 \dots i_N} &= Q(\mathcal{M}_{i_1 \dots i_N} + \epsilon_{i_1 \dots i_N}), \quad (i_1, \dots, i_N) \in \Omega \\ \epsilon_{i_1 \dots i_N} &\sim \text{Logistic}(0, 1) \quad \text{or} \quad \epsilon_{i_1 \dots i_N} \sim \mathcal{N}(0, 1) \end{aligned}$$

where $Q(\cdot) : \mathbb{R} \rightarrow \mathcal{F}$ is a uniform scalar quantizer that maps a real number to one of the P labels of $\mathcal{F} = \{1, \dots, P\}$ ($P = 2^{\text{bits of quantization}} - 1$), e.g.

$$Q(x) = p, \text{ if } w_{p-1} < x \leq w_p, \quad p \in \mathcal{F},$$

where $\{w_0, \dots, w_P\}$, $w_0 \leq \dots \leq w_P$ represents the set of quantization bin boundaries of all measurements (we assume that is known a priori).

Quantized Matrix Completion

We solve the following constrained optimization problem:

$$\begin{aligned} \text{minimize } \mathbf{M}_{(n)} & - \sum_{j,k:(j,k) \in \Omega_n} \log p(\mathbf{Y}_{(n)j,k} \mid \mathbf{M}_{(n)j,k}) \\ \text{subject to} & \quad \|\mathbf{M}_{(n)}\|_* \leq \lambda \end{aligned}$$

where $p(\mathcal{Y}_{i_1 \dots i_N} \mid \mathcal{M}_{i_1 \dots i_N}) = \Phi(\mathcal{U}_{i_1 \dots i_N} - \mathcal{M}_{i_1 \dots i_N}) - \Phi(\mathcal{L}_{i_1 \dots i_N} - \mathcal{M}_{i_1 \dots i_N})$, the $I_1 \times \dots \times I_N$ tensors \mathcal{U} and \mathcal{L} contain the upper and lower bin boundaries corresponding to the measurements.

The function $\Phi(x)$ corresponds to an inverse link function.

- Logistic model: $\Phi_{\log}(x) = \frac{1}{1+e^{-x}}$,
- Probit model: $\Phi_{\text{pro}}(x) = \int_{-\infty}^x \mathcal{N}(s \mid 0, 1) ds$.

Algorithm

Starting with the measurement matrix $\mathbf{Z}_{(n)}^1 = \mathbf{Y}_{(n)}$, the algorithm performs two steps at each iteration l until convergence or the maximum number of iterations:

1. Reduce the objective function:

$$\hat{\mathbf{Z}}_{(n)}^{l+1} \leftarrow \mathbf{Z}_{(n)}^l - s_l \cdot \nabla f,$$

where $s_l = \frac{1}{L}$ is the step-size ($L_{\log} = \frac{1}{4}$, $L_{\text{pro}} = 1$) and

$$[\nabla f]_{j,k} = \begin{cases} \frac{\phi'(\mathbf{L}_{(n)j,k} - \mathbf{Z}_{(n)j,k}) - \phi'(\mathbf{U}_{(n)j,k} - \mathbf{Z}_{(n)j,k})}{\phi(\mathbf{U}_{(n)j,k} - \mathbf{Z}_{(n)j,k}) - \phi(\mathbf{L}_{(n)j,k} - \mathbf{Z}_{(n)j,k})} & \text{if } (j, k) \in \Omega_n \\ 0 & \text{otherwise} \end{cases}$$

2. Impose low-rankness on $\mathbf{Z}_{(n)}$:

$$\mathbf{Z}_{(n)}^{l+1} \leftarrow \mathbf{U} \cdot \text{diag}(s) \cdot \mathbf{V}^T, \text{ with } s = P_\lambda(\text{diag}(\mathbf{S})),$$

where $\mathbf{U} \cdot \mathbf{S} \cdot \mathbf{V}^T$ denotes the singular value decomposition (SVD) of $\hat{\mathbf{Z}}_{(n)}^{l+1}$ and P_λ the projection onto the l_1 -ball with radius λ .

Dynamic weights

The estimated tensors \mathcal{I}_n is produced by folding each of the recovered matrices $\mathbf{Z}_{(n)}$ such that:

$$\mathcal{M} \approx \sum_{n=1}^N a_n \cdot \mathcal{I}_n$$

where

$$a_n = \frac{[\text{fit}_n(\mathbf{Z}_{(n)})]^{-1}}{N \sum_{i=1}^N [\text{fit}_i(\mathbf{Z}_{(i)})]^{-1}}, \quad n = 1, \dots, N$$

and the fitting error is given by

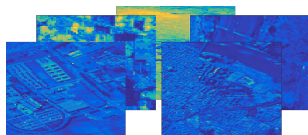
$$\text{fit}_n(\mathbf{Z}_{(n)}) = \|\mathcal{P}_\Omega(\text{fold}_n(\mathbf{Z}_{(n)}) - \mathcal{Y})\|_F.$$

The dynamic weights a_n can improve the recovery quality of the recovered tensor.

Experiments

Experimental results on publicly available hyperspectral Earth Observation images taken from airbornes or satellites over

- Indian Pines (14 bits per pixel)
- Botswana (14 bits per pixel)
- Pavia Center (13 bits per pixel)
- Pavia University (13 bits per pixel)
- Kennedy Space Center (16 bits per pixel)



To assess the recovery performance of our algorithm for different sampling percentages, we use

- The Normalized Mean Square Error - Lower is better
- The peak signal to noise ratio (PSNR) in decibels - Higher is better

Recovery error for each unfolding

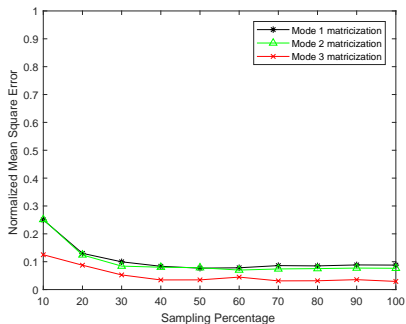
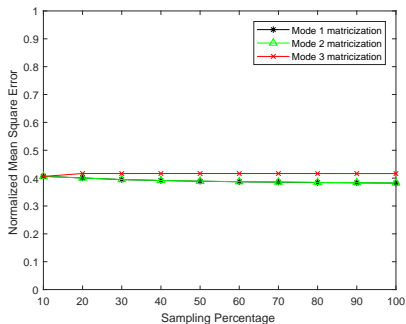


Figure: Normalized mean square error to each mode matricization on the hyperspectral image over Indian Pines, using the probit model and (left) 1 bit and (right) 6 bits for quantization.

Models

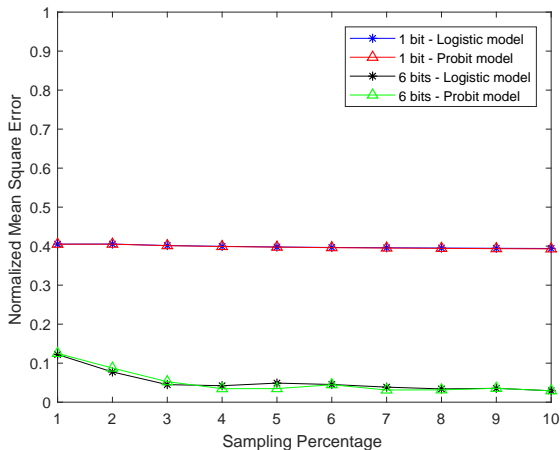


Figure: Normalized mean square error for each model, using 1 and 6 bits for quantization on the hyperspectral image over Indian Pines.

Bits of quantization

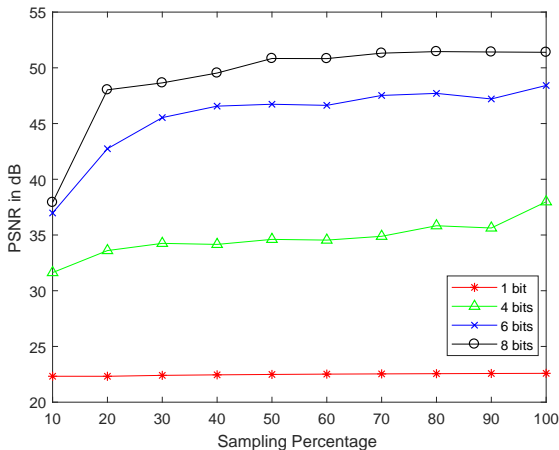


Figure: PSNR for each number of bits of quantization, using the probit model on the hyperspectral image over Indian Pines.

Recovery error for each hyperspectral image

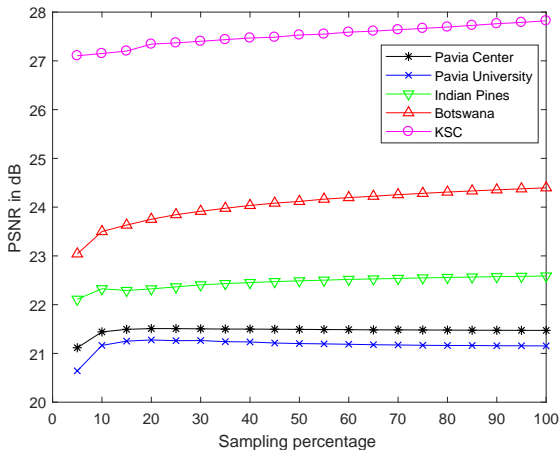


Figure: PSNR for each hyperspectral image, using the probit model and 1 bit for quantization.

Reconstructed images

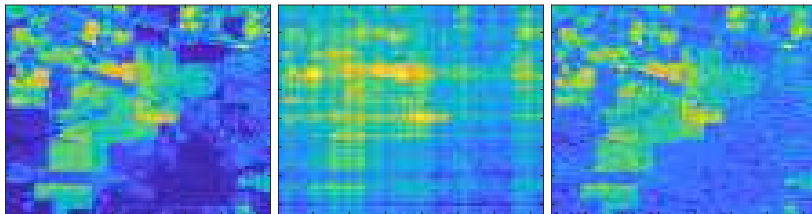


Figure: The original (left) and the reconstructed images of Indian Pines for 20% sampling percentage, using the probit model with 1 bit (middle) and 4 bits (right) for quantization.

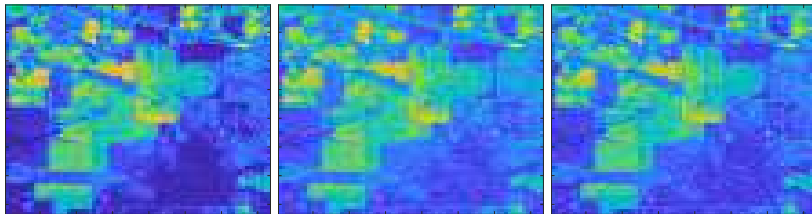


Figure: The original (left) and the reconstructed images of Indian Pines for 20% sampling percentage, using the probit model with 6 bits (middle) and 8 bits (right) for quantization.

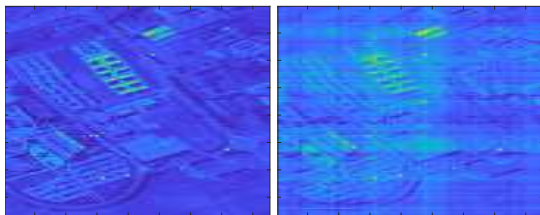


Figure: The original (left) and the reconstructed image (right) of Pavia University for 50% sampling percentage, using the probit model with 1 bit for quantization.

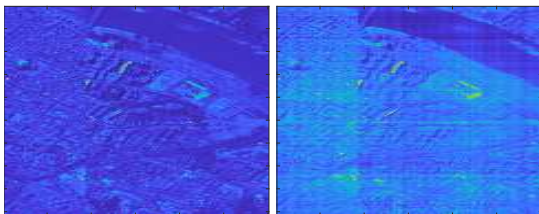
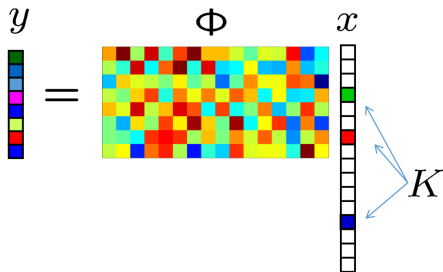


Figure: The original (left) and the reconstructed image (right) of Pavia Center for 50% sampling percentage, using the probit model with 1 bit for quantization.

Compressed Sensing

Goal: Recover a sparse signal $\mathbf{x} \in \mathbb{R}^N$ from measurements $\mathbf{y} \in \mathbb{R}^M$ with $M \ll N$.



Problem: Random projection $\Phi \in \mathbb{R}^{M \times N}$ not full rank (ill-posed inverse problem).

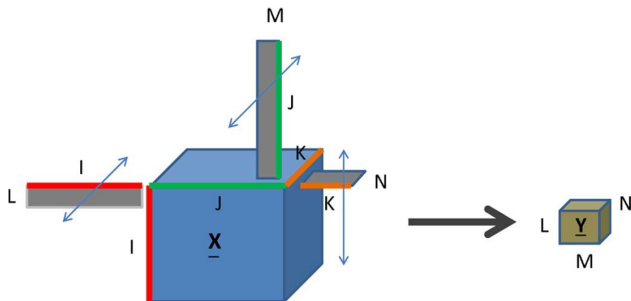
Solution: Exploit the sparse/compressible geometry of acquired signal \mathbf{x}

$$\hat{\mathbf{x}} = \operatorname{argmin}_{\mathbf{x}} \|\mathbf{x}\|_1 \text{ subject to } \Phi \mathbf{x} = \mathbf{y}$$

Compressed Sensing for Sparse Low-Rank Tensors 1/2

Sparse, low-rank tensor $\mathcal{X} \in \mathbb{R}^{I \times J \times K}$.

Much smaller measurement tensor $\mathcal{Y} \in \mathbb{R}^{L \times M \times N}$ which is obtained by multiplying (every slab of) \mathcal{X} from the I -mode with \mathbf{U}^T , from the J -mode with \mathbf{V}^T and from the K -mode with \mathbf{W}^T , where \mathbf{U} is $I \times L$, $L \leq I$, \mathbf{V} is $J \times M$, $M \leq J$ and \mathbf{W} is $K \times N$, $N \leq K$.



¹Reference: Sidiropoulos, N. D., and Kyrillidis, A. (2012). Multi-way compressed sensing for sparse low-rank tensors. IEEE Signal Processing Letters, 19(11), 757-760.

Compressed Sensing for Sparse Low-Rank Tensors 2/2

Recovery: Under some assumptions for the values of L, M, N , the original factor loadings $\mathbf{A}, \mathbf{B}, \mathbf{C}$ (matrices with columns the vectors whose outer products are the rank-one tensors that synthesize the tensor \mathcal{X}) are almost surely identifiable from the compressed data \mathcal{Y} up to a common column permutation and scaling.

It can be generalized to four and higher-way tensors.

¹*Reference:* Sidiropoulos, N. D., and Kyrillidis, A. (2012). Multi-way compressed sensing for sparse low-rank tensors. *IEEE Signal Processing Letters*, 19(11), 757-760.

*Thank
You!*